Editors' Suggestion

Physical Origin of Transient Negative Capacitance in a Ferroelectric Capacitor

Sou-Chi Chang,* Uygar E. Avci, Dmitri E. Nikonov, Sasikanth Manipatruni, and Ian A. Young
Components Research, Intel Corporation, Hillsboro, Oregon 97124, USA

(Received 30 August 2017; revised manuscript received 3 November 2017; published 10 January 2018)

Transient negative differential capacitance, the dynamic reversal of transient capacitance in an electrical circuit, is of highly technological and scientific interest since it probes the foundation of ferroelectricity. We study a resistor-ferroelectric capacitor (*R*-FEC) network through a series of coupled equations based on Kirchhoff's law, electrostatics, and Landau theory. We show that transient negative capacitance (NC) in a *R*-FEC circuit originates from the mismatch in switching rate between the free charge on the metal plate and the bound charge in a ferroelectric (FE) capacitor during the polarization switching. This transient free charge–polarization mismatch is driven by the negative curvature of the FE free-energy landscape, and it is also analytically shown that a free-energy profile with a negative curvature is the only physical system that can describe transient NC in a *R*-FEC circuit. Furthermore, transient NC induced by the free charge–polarization mismatch is justified by its dependence on both external resistance and the intrinsic FE viscosity coefficient. The depolarization effect on FE capacitors emphasizes the importance of negative curvature to transient NC and also implies that transient and steady-state NC cannot be observed in a FE capacitor simultaneously. Finally, using the transient NC measurements, a procedure to experimentally determine the viscosity coefficient is presented to provide more insight into the relation between transient NC and the FE free-energy profile.

DOI: 10.1103/PhysRevApplied.9.014010

I. INTRODUCTION

In the past four decades, the computing power of microprocessors has been significantly improved due to the relentless pursuit of Moore's law [1]. However, the static power becomes increasingly important in the total energy dissipation as the CMOS transistors in a microchip are scaled down to the nanometer regime due to the reduction of the on-off current ratio [2]. Recently, an alternative gate structure based on the ferroelectric (FE) oxide [also known as a negative-capacitance (NC) field-effect transistor] was proposed for transistors to improve the on-off current ratio by enhancing depolarization fields along the gate stack [3,4]. The main idea behind this approach is that the enhancement of gate capacitance is realized by the elimination of negative curvature in the FE thermodynamic profile through depolarization, which can be achieved by engineering the ratio between dielectric (DE) and FE thicknesses in the gate stack [4]. Therefore, it is of great importance to experimentally show the existence of negative curvature between two stable polarization states in the thermodynamic free-energy profile in FE materials predicted by Landau theory.

A FE capacitor is an excellent device to study the FE free-energy profile due to its simple structure. There are two types of NC in a FE capacitor that have been extensively discussed in the literature [4–7]. One is known as nontransient (or steady-state) NC, which is a result of the depolarization-driven capacitance enhancement accomplished by stabilizing the polarization in the region of negative curvature in the FE free-energy profile [4,7]. This nontransient NC is typically achieved in a FE-DE capacitor; thus, capacitance enhancement refers to the increase in capacitance of the FE-DE stack compared to that associated only with the DE layer. Note that this steady-state NC cannot be directly measured due to thermodynamic stability, and it therefore can be deduced only from the capacitance enhancement of a FE-DE stack based on the DE layer.

Another NC in a FE capacitor is known as transient negative differential capacitance (or transient NC), which, in general, refers to a transient response of a FE capacitor in a *R*-FEC circuit, where charge on a capacitor increases while the voltage across the capacitor is reduced [5,6]. Recently, it was claimed that this transient NC can be viewed as a direct mapping to the negative curvature of the FE free-energy profile during polarization switching [5,6]. However, thus far, there have been no clear physical or theoretical descriptions to directly link transient NC to the negative curvature of a FE free-energy profile. Hence, it is of great importance to establish (i) a correct physical picture for the transient NC measured in a *R*-FEC circuit [5,6] and also (ii) the relation between transient NC and the negative curvature of the FE free-energy landscape. In this

*sou-chi.chang@intel.com

paper, we show that transient NC measured in a R-FEC circuit originates from the mismatch in switching rate between the free charge on the metal plate and the bound charge in a FE capacitor during polarization switching, which is driven by the negative curvature of the FE thermodynamic energy profile. Analytical expressions are also established to prove that the negative curvature in the free-energy profile is the only solution that can physically describe transient NC during the two-state switching in a R-FEC circuit. Also, transient NC induced by this free charge–polarization mismatch is justified by the dependence of transient NC on both the external resistance and the intrinsic viscosity coefficient. Furthermore, the depolarization effect in a FE capacitor shows that the negative curvature in the free-energy profile is required to observe transient NC; thus, transient and steady-state NC cannot coexist in a FE capacitor.

This paper is organized as follows. In Sec. II, a theoretical formalism to describe free charge and polarization dynamics in a R-FEC circuit is presented in detail. Based on the model, in Sec. III, the physical origin of transient NC in a R-FEC circuit and the corresponding thermodynamic picture are explained. Also, the effects of external resistance, the intrinsic viscosity coefficient, and the depolarization field on a FE capacitor are discussed. Furthermore, a procedure to determine the viscosity coefficient directly from the transient NC measurements is given to gain more insight from polarization dynamics. Section IV concludes the paper.

II. THEORETICAL FORMALISM

To describe the dynamics for both free charge and polarization in the R-FEC circuit shown in Fig. 1, (i) Kirchhoff's law is used to describe the displacement current flowing through the external resistor, (ii) electrostatics is applied because the net charge on a FE capacitor has to be equal to free charge plus bound charge, and (iii) average polarization dynamics under an electric field across the FE oxide is captured by Landau theory. The equation corresponding to Kirchhoff's law is given as

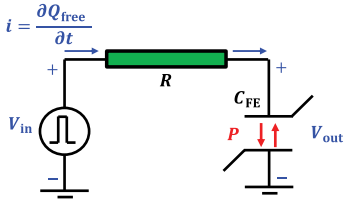

FIG. 1. The schematic of a resistance-ferroelectric capacitor (R-FEC) circuit for studying the physical origin of transient NC observed in the experiments in Refs. [5,6]. V_{in}, V_{out} are the input and output voltages, respectively, R is the external resistance, and C_{FE} is the ferroelectric capacitor. The current flowing through the resistor is determined by the first-order time derivative of the free charge, Q_{free}.

$$\frac{\partial Q_{free}}{\partial t} = \frac{V_{in} - V_{out}}{RA} = \frac{V_{in} - V_{FE}}{RA}, \tag{1}$$

where $\partial Q_{free}/\partial t$ is the displacement current density (A/m^2), V_{in} and V_{out} are the input and output voltages (in volts), respectively, R is the external resistance (in ohms), and A is the area of a capacitor (in m^2). Note that V_{out} is equal to V_{FE}, which is the voltage across a FE capacitor. Based on the electrostatics, the free charge density (Q_{free}) on a FE capacitor can be written as

$$Q_{free} = \epsilon_0 E_{FE} + P, \tag{2}$$

where E_{FE} is the electric field across the FE oxide, ϵ_0 is the vacuum dielectric constant, and P is the average FE polarization [8–10], whose dynamics is governed by the Landau theory given as [10–14]

$$\gamma \frac{\partial P}{\partial t} = -\left(2\alpha_1 + \frac{t_{dep}}{\epsilon_0 t_{FE}}\right) P - 4\alpha_{11} P^3 - 6\alpha_{111} P^5 + E_{FE}, \tag{3}$$

where α_1, α_{11}, and α_{111} are thermodynamic expansion coefficients for the bulk FE free energy, γ is the viscosity coefficient, and t_{FE} and t_{dep} are FE oxide and effective depolarization thicknesses, respectively. Note that t_{dep} is used to represent the depolarization effect associated with the finite screening length of metal contacts and the inevitable interface dead layers in a FE capacitor; that is, $t_{dep} = (\lambda_1/\epsilon_1) + (\lambda_2/\epsilon_2) + (t_{DE}/\epsilon_{DE})$, with λ_1, λ_2, and t_{DE} being the screening lengths of the top and bottom metal contacts and the dead-layer thickness, respectively, and ϵ_1, ϵ_2, and ϵ_{DE} being the relative dielectric constants of the top and bottom contacts and the dead layer, respectively [15]. By combining Eqs. (1)–(3), the differential equation for free charge dynamics in a R-FEC circuit is given as

$$RA \frac{\partial Q_{free}}{\partial t} = V_{in} - \frac{t_{FE}(Q_{free} - P)}{\epsilon_0}. \tag{4}$$

From Eqs. (3) and (4), one can immediately see that free charge and polarization are coupled through the electric field across the FE oxide. Also, the free charge and polarization responses are limited by the external resistance and the intrinsic viscosity coefficient, respectively.

III. RESULTS AND DISCUSSION

Based on the mathematical model presented in the preceding section, the underlying physics behind transient NC in a R-FEC circuit is discussed in this section. The simulation parameters are summarized in Table I if not mentioned elsewhere. Equations (3) and (4) are integrated numerically using the Euler method, and the time step is chosen such that the results remain unchanged for a shorter time step. Note that, for all of the simulation results shown below, a negative input voltage is initially applied on the capacitor to set the polarization in the negative direction.

TABLE I. Simulation parameters for a *R*-FEC circuit.

Symbol	Quantity	Value
α_1		-1.05×10^9 m/F [16]
α_{11}	Landau expansion coefficient	10^7 m^5/C^{2}F [16]
α_{111}		6×10^{11} m^9/C^{4}F [16]
t_{dep}	Effective depolarization thickness	0.05 nm
t_{FE}	Ferroelectric thickness	10 nm
A	Capacitor area	50^2 μm^2
R	External resistance	50 kΩ
γ	Viscosity coefficient	5×10^2 m sec /F

A. Transient negative capacitance due to free charge–polarization mismatch

Figure 2(a) shows the output response in a *R*-FEC circuit under an input pulsed signal. The free charge on a FE capacitor is also given in the same figure. From Fig. 2(a), it can be seen that there are two regions where the free charge is increased (decreased) but the voltage is decreased (increased); that is, $(\partial Q_{free}/\partial V) < 0$. This negative differential capacitance occurs only during the polarization reversal, which can be seen for the same time scale in Fig. 2(b), where both free charge and polarization as functions of time are given. Figure 2(b) also indicates that the free charge and polarization are almost equal in a *R*-FEC circuit under a pulsed input. However, Fig. 2(c) shows that there always exists a small difference between free charge and polarization in the ramping rate while charging a FE capacitor, and $(\partial P/\partial t) > (\partial Q_{free}/\partial t)$ occurs only when the polarization is switched. From Eq. (5), it can be seen that how the voltage across a FE capacitor changes with time is linearly proportional to the mismatch in switching rate between free charge and polarization.

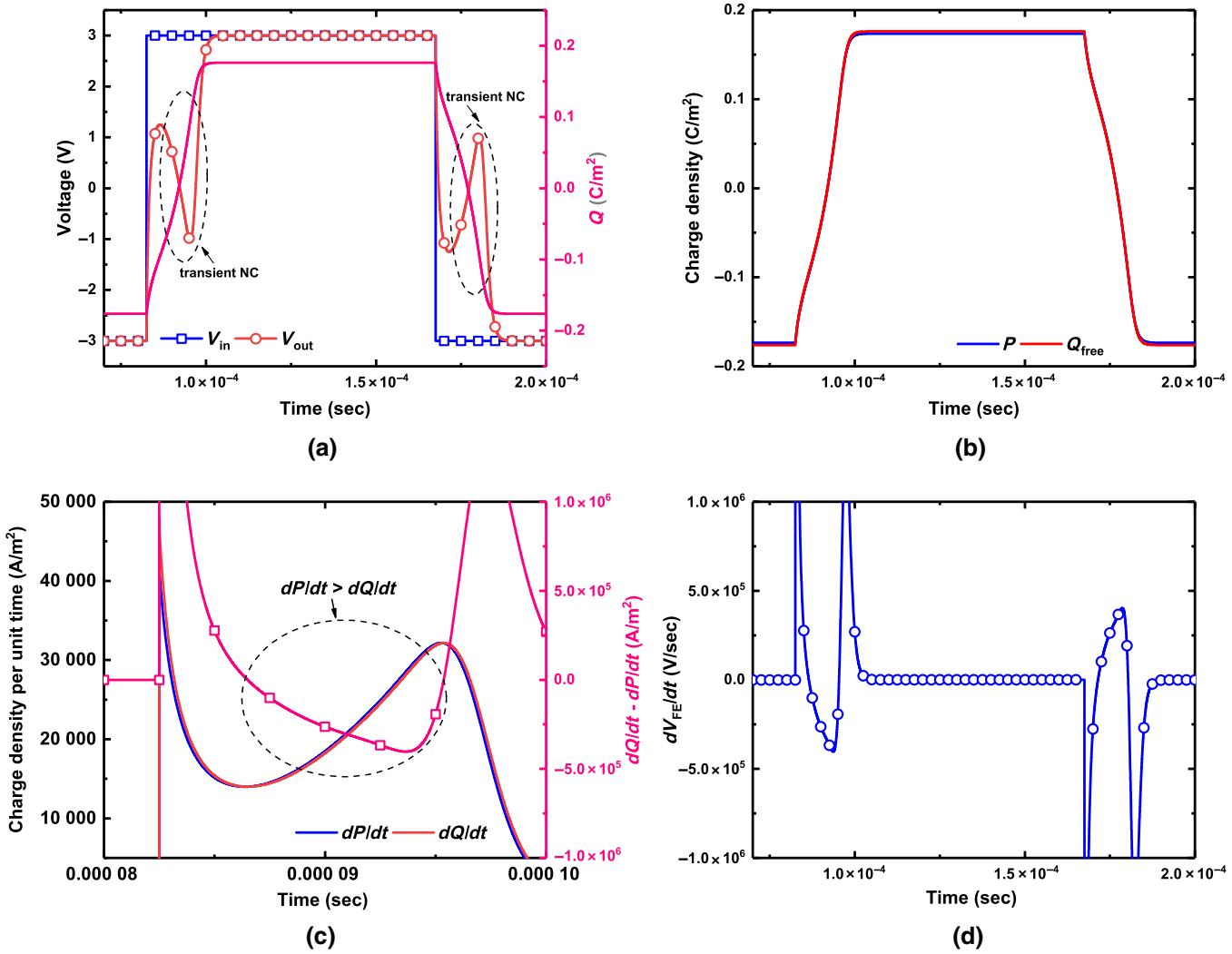

FIG. 2. (a) Input voltage (blue), output voltage (red), and free charge on a FE capacitor (pink) as functions of time. (b) Polarization and free charge as functions of time. (c) Charge density per unit time for free charge (red) and polarization (blue). The difference between $(\partial Q/\partial t)$ and $(\partial P/\partial t)$ is shown in pink. (d) Change in the voltage across a FE capacitor per unit time as a function of time.

Also, by comparing Figs. 2(a) and 2(d), it can be clearly seen that transient NC shows up exactly when $(\partial V_{\mathrm{FE}}/\partial t)$ becomes negative, which can be physically explained by the fact that the polarization starts changing faster than the free charge during the polarization switching [4,17]. Note that the response time scales for both the free charge and the polarization in a R-FEC circuit are of the same order of magnitude, as can be seen in Fig. 2(b). This is the case because Eqs. (3) and (4) indicate that both the free charge and the polarization dynamics are limited by the electric field across the FE capacitor, which is again determined by both the free charge and the polarization:

$$\frac{\partial V_{\mathrm{FE}}}{\partial t} = \frac{t_{\mathrm{FE}}}{\epsilon_0}\left(\frac{\partial Q_{\mathrm{free}}}{\partial t} - \frac{\partial P}{\partial t}\right). \tag{5}$$

Next, the relation between the free charge–polarization mismatch and the negative curvature of the thermodynamic profile is established. Figure 3(a) shows that transient NC occurs when the polarization is in the negative curvature region of the thermodynamic energy profile. This correlation can be also seen in Fig. 3(b), where the thermodynamic profiles at different time steps are given while charging a FE capacitor. From Fig. 3(b), we determine that the FE free-energy profile is always changing, as the free charge is built up across the capacitor. Therefore, Fig. 1 in Ref. [5] does not provide a rigorous physical picture to describe transient NC in a R-FEC circuit, where the free-energy profile under a fixed bias is used for the explanation of transient NC. Note that, in Fig. 3(a), the corresponding negative curvature in the region of transient NC can be considered a direct mapping of the negative curvature in the free-energy profile under equilibrium since, in Eq. (3), it can be immediately seen that $(\partial^2 P/\partial U^2)$ has no dependence on the electric field across the FE capacitor. Furthermore, in Eq. (5), it can be seen directly that when a capacitor is charged with a positive input voltage, transient NC appears when $(\partial P/\partial t) > (\partial Q_{\mathrm{free}}/\partial t) > 0$ is satisfied. On the other hand, $(\partial P/\partial t) < (\partial Q_{\mathrm{free}}/\partial t) < 0$ is required for transient NC as a negative input voltage is applied in a R-FEC circuit.

Based on Landau theory ($\gamma(\partial P/\partial t) = -(\partial U/\partial P)$, with U being the free energy), $(\partial V_{\mathrm{FE}}/\partial t)$, at a given time t_0, can be connected to the curvature of the thermodynamic energy profile,

$$\begin{aligned}\left.\frac{\partial V_{\mathrm{FE}}}{\partial t}\right|_{t=t_0} &= \frac{t_{\mathrm{FE}}}{\epsilon_0}\left(\left.\frac{\partial Q_{\mathrm{free}}}{\partial t}\right|_{t=t_0} + \left.\frac{\partial U}{\gamma \partial P}\right|_{t=t_0}\right) \\ &= \frac{t_{\mathrm{FE}}}{\epsilon_0}\left(\left.\frac{\partial Q_{\mathrm{free}}}{\partial t}\right|_{t=t_0} + \left.\frac{\partial U}{\gamma \partial P}\right|_{P=P_i} + \frac{1}{\gamma}\int_{P_i}^{P_{t=t_0}} \frac{\partial^2 U}{\partial^2 P} dP\right),\end{aligned} \tag{6}$$

where P_i and $P_{t=t_0}$ are the initial polarization and polarization at $t = t_0$. In Eq. (6), one can immediately see that

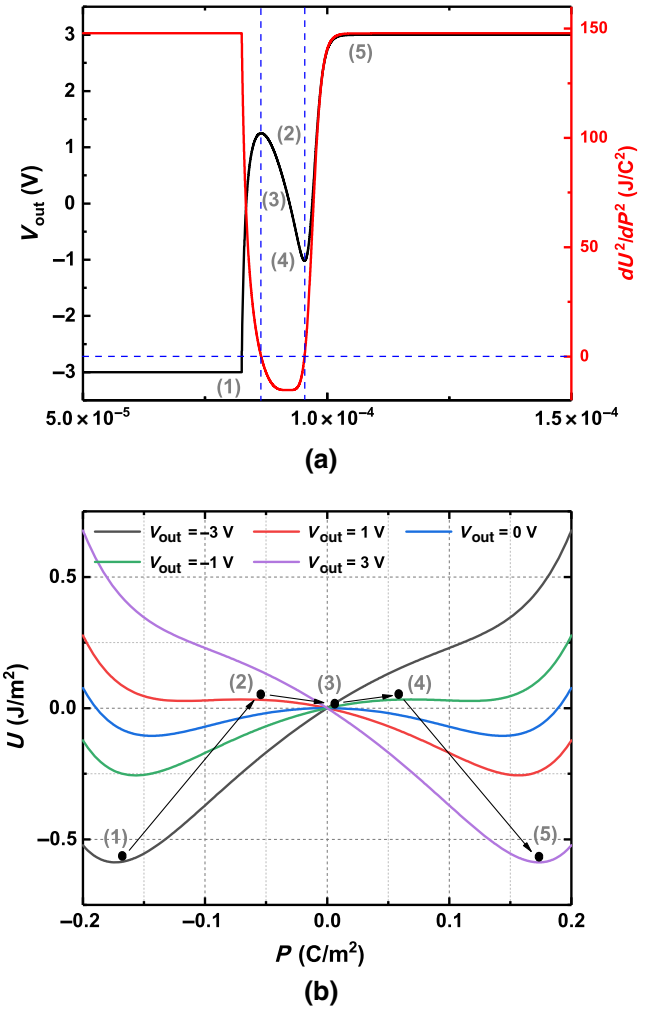

FIG. 3. (a) Output voltage and curvature of the FE thermodynamic free-energy profile as functions of time. The sign reversal of $(\partial V_{\mathrm{out}}/\partial t)$ coincides with $(\partial^2 U/\partial P^2) < 0$. (b) The thermodynamic free-energy profiles at different time steps when charging a FE capacitor. The black dots and the arrows connecting the black dots represent transient polarization states and switching directions, respectively. The parameters are the same as those in Fig. 2.

there are only two possible situations [Eqs. (7) and (8)] for a two-state system that can satisfy the conditions for transient NC mentioned above:

$$\text{(i)}\quad \left.\frac{\partial^2 U}{\partial^2 P}\right|_{t=t_0} < 0, \quad \text{for } P_i < P(t=t_0) \text{ and } V_{\mathrm{in}} > 0 \quad \text{for } P_i > P(t=t_0) \text{ and } V_{\mathrm{in}} < 0, \tag{7}$$

$$\text{(ii)}\quad \left.\frac{\partial^2 U}{\partial^2 P}\right|_{t=t_0} > 0, \quad \text{for } P_i > P(t=t_0) \text{ and } V_{\mathrm{in}} > 0 \quad \text{for } P_i < P(t=t_0) \text{ and } V_{\mathrm{in}} < 0. \tag{8}$$

In Eqs. (7) and (8), it can be seen that only condition (i) can physically describe polarization switching when charging a

FE capacitor in a R-FEC circuit. As a result, the measured transient NC in a R-FEC circuit can be considered strong evidence for the existence of negative curvature in the FE thermodynamic profile.

B. Effects of external resistance, intrinsic viscosity coefficient, and depolarization field

As mentioned above, transient NC in a R-FEC circuit is due to the difference between the polarization and the free charge in the charging rate, while the polarization is reversed. It is intuitive to expect that both the external resistance and the intrinsic FE viscosity coefficient can play significant roles in transient NC as well. Figure 4(a) illustrates the effects of external resistance on transient NC. From Fig. 4(a), it is found that, as the external resistance becomes larger, the polarization switching is slower since it takes more time for the free charge to build up the electric field across a FE capacitor. More importantly, transient NC becomes more pronounced with larger external resistance due to a decreasing $\partial Q_{\text{free}}/\partial t$ value [or an increase of the mismatch in Eq. (5)]. On the other hand, the mismatch can also be enhanced by speeding up the polarization switching as shown in Fig. 4(b), where a smaller viscosity coefficient refers to faster switching dynamics.

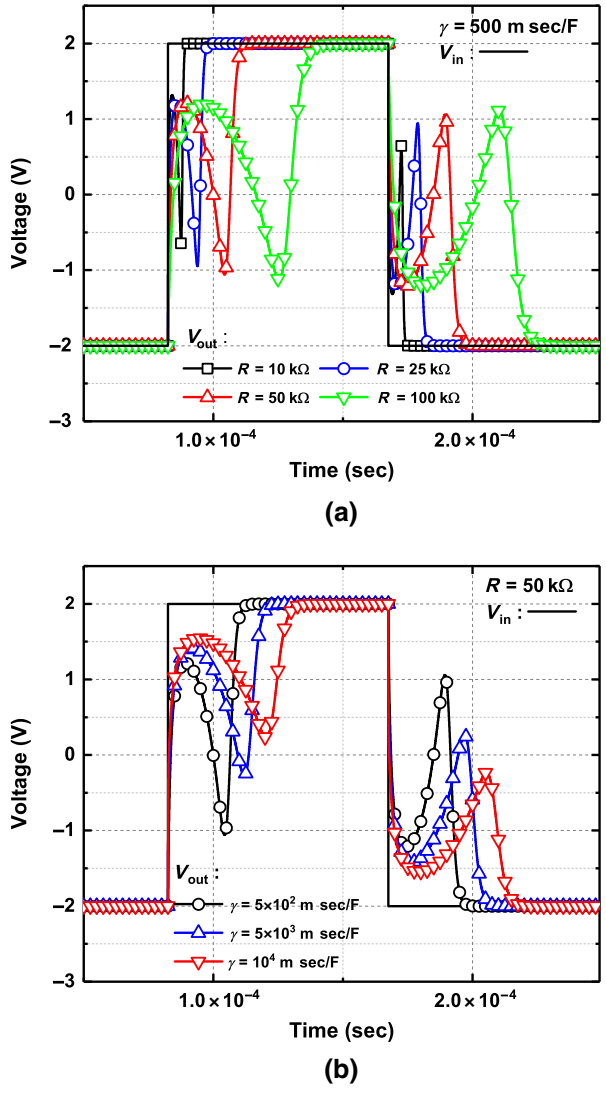

FIG. 4. The effect of (a) the external resistance and (b) the viscosity coefficient on transient negative capacitance in a R-FEC circuit.

Thus far, we have analytically shown that the negative curvature is required to induce the mismatch between polarization and free charge (transient NC) in a R-FEC circuit; that is, Eqs. (6)–(8). Consequently, we also expect the depolarization effect on a FE capacitor to affect transient NC significantly. It is well known that, as the FE oxide gets thinner in a capacitor, the depolarization effect becomes more pronounced in degrading the ferroelectricity in the material [18]. As a result, $\partial P/\partial t$ becomes less important in Eq. (5), with a stronger depolarization field, and transient NC is thus weaker [as shown in Fig. 5(a)]. Note that transient NC can be totally removed when the depolarization field is strong enough. In Fig. 5(b), it can be seen that the elimination of transient NC corresponds to the transition from a two-state to a single-state system, which again emphasizes the importance of negative curvature to the FE thermodynamic energy profile.

In Fig. 5(b), the free-energy profile of a thin dead layer ($t_{\text{dep}} = 0.05$ nm, gray curve) is also included to show that the capacitance (approximately $1/(\partial^2 U/\partial P^2)$) can be enhanced when we have a thin FE layer in the stack (blue curve), and, under such a situation, capacitance associated with the FE layer is effectively negative in the stack, as explained in Refs. [4,7]. This type of NC is nontransient because the depolarization effect is strong enough to make the free-energy profile thermodynamically stable (i.e., double well to parabola), while the polarization is able to stay in the negative curvature of the FE. Consequently, the transient and nontransient NC cannot coexist in the same FE capacitor since, in the free-energy profile, the former requires the existence of negative curvature to be observed and it is necessary to eliminate the negative curvature to stabilize the latter.

C. Viscosity coefficient extracted from transient NC measurements

As mentioned in Sec. II, the dynamics of average polarization in the FE is described by Eq. (3). In general, FE polarization dynamics driven by an external electric field is mostly dominated by incoherent processes such as domain nucleation and propagation [19,20]. Therefore, we can expect a polarization-dependent viscosity coefficient that reflects all of the domain-related effects in Eq. (3). By using the transient NC measurements, the viscosity coefficient can be experimentally determined, and the procedure is given in detail below. Note that the experimental

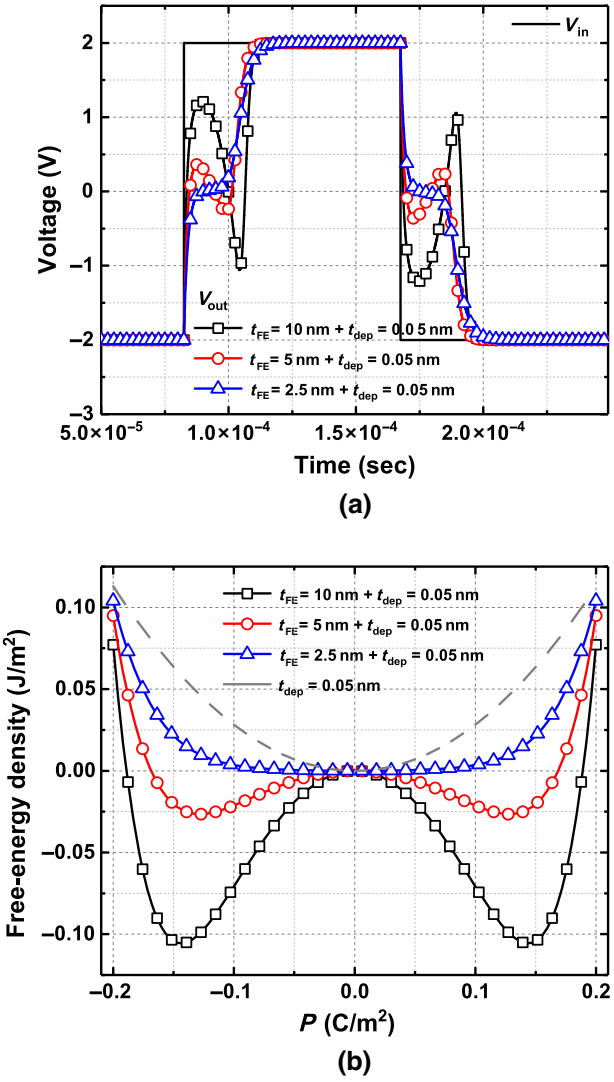

FIG. 5. (a) Input and output voltages as functions of time with different FE thicknesses ($t_{dep} = 0.05$ nm). (b) Thermodynamic free-energy profile of FE with different FE thicknesses ($t_{dep} = 0.05$ nm).

results we use here are from Ref. [21], where FE capacitors based on doped hafnium oxide are studied.

From the transient NC measurements, $\partial Q_{free}/\partial t$ and $\partial V_{FE}/\partial t$ can be directly obtained by recording the current flowing through the external resistance and the voltage across the FE capacitor (see, e.g., Figs. 12 and 13 in Ref. [21]), and thus $\partial P_{free}/\partial t$ can be extracted, based on Eq. (5). The amount of polarization switched under a given voltage pulse, ΔP, can be calculated by integrating $\partial P_{free}/\partial t$ over time (i.e., $\Delta P = \int_0^t (\partial P_{free}/\partial t')dt'$). Since, in the transient NC measurements, the voltage pulse is typically applied long enough that the electrical response of the FE capacitors reaches the steady state. Therefore, the final polarization under a long voltage pulse, P_f, can be deduced by finding the polarization at the energy minimum in the steady-state free-energy profile (i.e., $(\partial U/\partial P) = 0$), which can be determined by experimentally fitting the frequency-independent hysteresis loop (i.e., Fig. 11 in Ref. [21]), and the initial polarization before the voltage pulse is switched, P_i, can be simply calculated using $P_i = P_f - \Delta P$. Once the polarization evolution during transient NC measurements is obtained from the experiments, it is straightforward to calculate the viscosity coefficient using Landau theory [i.e., $\gamma = -(\partial U/\partial P)/(\partial P/\partial t)$].

Based on the procedure mentioned above, Fig. 6(d) shows the viscosity coefficient extracted from the transient NC measurements in Ref. [21]. The steady-state free-energy profile determined by fitting the frequency-independent hysteresis loop is also given in Figs. 6(a) and 6(b). The calculated switching polarization profile based on the transient NC measurements is shown in Fig. 6(c). In Fig. 6(d), it can be seen that the extracted viscosity coefficient is polarization dependent, which is expected since Eq. (3) is used to describe the average polarization of the FE thin film, and all domain-related effects are thus incorporated into the viscosity coefficient. In Fig. 6(d), it can be seen that the viscosity coefficient increases with the amount of switched polarization, which we can explain using the fact that the switching process becomes slower as more FE domains are involved in the dynamics. Also, one can observe that the viscosity coefficient starts and ends with much lower values than those during polarization switching. This finding can be attributed to the fact that the dielectric response is much faster than the FE domain dynamics in the thin film; therefore, when the voltage across the FE capacitor is not strong enough to switch FE domains or when most of the FE domains are already switched under a given voltage pulse, the dynamics is then determined by the dielectric response rather than the domain motion. Note that, based upon the experimental results shown in Ref. [21], where only one pulse period is used for the measurements, it is impossible to distinguish whether the domain dynamics is dominated by nucleation only [22–24] or by both nucleation and propagation [25,26] from the extracted viscosity coefficient. This is the case because, to identify the detailed domain-switching mechanism, a pulse period spanning four to eight decades is typically required (see, e.g., Fig. 2 in Ref. [22] and Fig. 1 in Ref. [24]); therefore, more experimental results are needed to clarify the relation between the extracted viscosity coefficient and the detailed domain-switching mechanism, which is beyond the scope of this paper.

Next, in Figs. 6(b) and 6(c), it can be seen that transient NC measured in the experiment occurs only in the partial region of negative curvature in the free-energy profile, not in the perfect mapping shown in Figs. 3(a) and 3(b). This difference can be attributed to the following causes. (i) The viscosity coefficient increases as more FE domains are reversed; therefore, the second term in Eq. (5), which is inversely proportional to γ, becomes less important when the polarization dynamics is slower. Consequently, in Eq. (5), the sign of $\partial V_{FE}/\partial t$ cannot be opposite that of $\partial Q_{free}/\partial t$, even though the curvature is negative if the

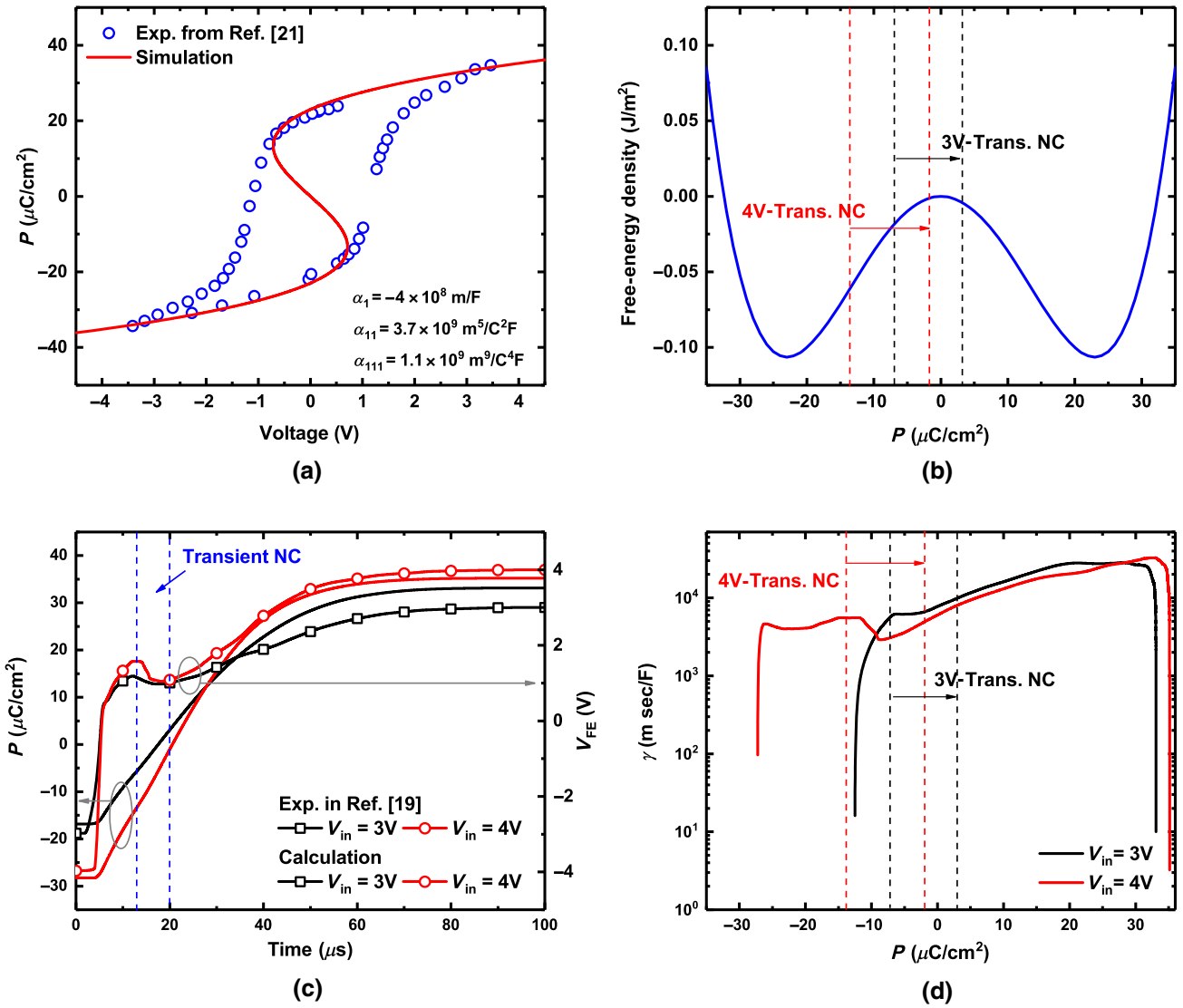

FIG. 6. (a) Measured frequency-independent hysteresis loop in Ref. [21] fitted by a steady-state LK equation without a depolarization field and (b) the corresponding FE free-energy profile under equilibrium. (c) Transient NC measured in Ref. [21] and the calculated switching polarization profile. (d) Extracted viscosity coefficient from (b) and (c) based on Landau theory.

viscosity coefficient is too large. (ii) The extracted viscosity coefficient from the experiment is about 1 to 2 orders of magnitude larger than that used in the simulation. Hence, the transient NC is less sensitive to the free-energy profile with larger viscosity coefficients, as can also be seen in Fig. 4(b). However, since the extracted viscosity coefficient is always positive, the transient NC can still be considered direct evidence for the existence of negative curvature in the free-energy profile, as indicated by Eq. (5).

IV. CONCLUSION

In summary, this paper shows that the physical origin of transient NC in a R-FEC circuit is induced by the mismatch of charging rate between the free charge and the FE bound charge during polarization switching, which is driven by the negative curvature of the thermodynamic profile. It is proved analytically that the negative curvature is the only solution that can physically describe the charging behavior of a FE capacitor in a R-FEC circuit. Furthermore, the dependence of the resistance, the viscosity coefficient, and the depolarization on transient NC is shown to justify the importance of the free charge–polarization mismatch and the negative curvature of the thermodynamic profile to transient NC. Finally, a procedure to experimentally determine the viscosity coefficient from the transient NC measurements is presented to provide more insight into the polarization dynamics.

[1] G. E. Moore, Cramming more components onto integrated circuits, Proc. IEEE **86**, 82 (1998).

[2] N. S. Kim, T. Austin, D. Baauw, T. Mudge, K. Flautner, J. S. Hu, M. J. Irwin, M. Kandemir, and V. Narayanan, Leakage current: Moore's law meets static power, Computer **36**, 68 (2003).
[3] Sayeef Salahuddin and Supriyo Datta, Use of negative capacitance to provide voltage amplification for low power nanoscale devices, Nano Lett. **8**, 405 (2008).
[4] S. C. Chang, U. E. Avci, D. E. Nikonov, and I. A. Young, A thermodynamic perspective of negative-capacitance field-effect transistors, IEEE J. Explor. Solid-State Comput. Devices Circuits **3**, 56 (2017).
[5] Asif Islam Khan, Korok Chatterjee, Brian Wang, Steven Drapcho, Long You, Claudy Serrao, Saidur Rahman Bakaul, Ramamoorthy Ramesh, and Sayeef Salahuddin, Negative capacitance in a ferroelectric capacitor, Nat. Mater. **14**, 182 (2015).
[6] Michael Hoffmann, Milan Pei, Korok Chatterjee, Asif I. Khan, Sayeef Salahuddin, Stefan Slesazeck, Uwe Schroeder, and Thomas Mikolajick, Direct observation of negative capacitance in polycrystalline ferroelectric HfO_2, Adv. Funct. Mater. **26**, 8643 (2016).
[7] Pavlo Zubko, Jacek C. Wojdel, Marios Hadjimichael, Stephanie Fernandez-Pena, Anais Sene, Igor Lukyanchuk, Jean-Marc Triscone, and Jorge Iniguez, Negative capacitance in multidomain ferroelectric superlattices, Nature (London) **534**, 524 (2016).
[8] G. Gerra, A. K. Tagantsev, and N. Setter, Ferroelectricity in Asymmetric Metal-Ferroelectric-Metal Heterostructures: A Combined First-Principles–Phenomenological Approach, Phys. Rev. Lett. **98**, 207601 (2007).
[9] A. K. Tagantsev, G. Gerra, and N. Setter, Short-range and long-range contributions to the size effect in metal-ferroelectric-metal heterostructures, Phys. Rev. B **77**, 174111 (2008).
[10] Yang Liu, Xiaojie Lou, Manuel Bibes, and Brahim Dkhil, Effect of a built-in electric field in asymmetric ferroelectric tunnel junctions, Phys. Rev. B **88**, 024106 (2013).
[11] R. Kretschmer and K. Binder, Surface effects on phase transitions in ferroelectrics and dipolar magnets, Phys. Rev. B **20**, 1065 (1979).
[12] S. C. Chang, S. Manipatruni, D. E. Nikonov, and I. A. Young, Clocked domain wall logic using magnetoelectric effects, IEEE J. Explor. Solid-State Comput. Devices Circuits **2**, 1 (2016).
[13] Yubo Qi and Andrew M. Rappe, Designing Ferroelectric Field-Effect Transistors Based on the Polarization-Rotation Effect for Low Operating Voltage and Fast Switching, Phys. Rev. Applied **4**, 044014 (2015).
[14] G. Vizdrik, S. Ducharme, V. M. Fridkin, and S. G. Yudin, Kinetics of ferroelectric switching in ultrathin films, Phys. Rev. B **68**, 094113 (2003).
[15] Sou-Chi Chang, Azad Naeemi, Dmitri E. Nikonov, and Alexei Gruverman, Theoretical Approach to Electro-resistance in Ferroelectric Tunnel Junctions, Phys. Rev. Applied **7**, 024005 (2017).
[16] A. Aziz, S. Ghosh, S. Datta, and S. K. Gupta, Physics-based circuit-compatible spice model for ferroelectric transistors, IEEE Electron Device Lett. **37**, 805 (2016).
[17] Gustau Catalan, David Jimenez, and Alexei Gruverman, Ferroelectrics: Negative capacitance detected, Nat. Mater. **14**, 137 (2015).
[18] A. Stamm, D. J. Kim, H. Lu, C. W. Bark, C. B. Eom, and A. Gruverman, Polarization relaxation kinetics in ultrathin ferroelectric capacitors, Appl. Phys. Lett. **102**, 092901 (2013).
[19] Rolf Landauer, Electrostatic considerations in $BaTiO_3$ domain formation during polarization reversal, J. Appl. Phys. **28**, 227 (1957).
[20] J. Li, B. Nagaraj, H. Liang, W. Cao, Chi. H. Lee, and R. Ramesh, Ultrafast polarization switching in thin-film ferroelectrics, Appl. Phys. Lett. **84**, 1174 (2004).
[21] M. Kobayashi, N. Ueyama, K. Jang, and T. Hiramoto, Experimental study on polarization-limited operation speed of negative capacitance FET with ferroelectric HfO_2, in *Proceedings of the 2016 IEEE International Electron Devices Meeting (IEDM), San Francisco, 2016* (IEEE, New York, 2016), p. 12.3.1, http://ieeexplore.ieee.org/document/7838402/.
[22] Alexander K. Tagantsev, Igor Stolichnov, Nava Setter, Jeffrey S. Cross, and Mineharu Tsukada, Non–Kolmogorov-Avrami switching kinetics in ferroelectric thin films, Phys. Rev. B **66**, 214109 (2002).
[23] O. Lohse, M. Grossmann, U. Boettger, D. Bolten, and R. Waser, Relaxation mechanism of ferroelectric switching in $Pb(Zr, Ti)O_3$ thin films, J. Appl. Phys. **89**, 2332 (2001).
[24] J. Y. Jo, H. S. Han, J.-G. Yoon, T. K. Song, S.-H. Kim, and T. W. Noh, Domain Switching Kinetics in Disordered Ferroelectric Thin Films, Phys. Rev. Lett. **99**, 267602 (2007).
[25] Vladimir Shur, Evgenii Rumyantsev, and Sergei Makarov, Kinetics of phase transformations in real finite systems: Application to switching in ferroelectrics, J. Appl. Phys. **84**, 445 (1998).
[26] Aya Seike, Kazushi Amanuma, Sota Kobayashi, Toru Tatsumi, Hiroki Koike, and Hiromitsu Hada, Polarization reversal kinetics of a lead zirconate titanate thin-film capacitor for nonvolatile memory, J. Appl. Phys. **88**, 3445 (2000).